JACS
JOURNAL OF THE AMERICAN CHEMICAL SOCIETY
Communication
pubs.acs.org/JACS

Conformational Locking by Design: Relating Strain Energy with Luminescence and Stability in Rigid Metal–Organic Frameworks

Natalia B. Shustova,[†] Anthony F. Cozzolino,[†] and Mircea Dincă*

Department of Chemistry, Massachusetts Institute of Technology, Cambridge, Massachusetts 02139, United States

Supporting Information

ABSTRACT: Minimization of the torsional barrier for phenyl ring flipping in a metal–organic framework (MOF) based on the new ethynyl-extended octacarboxylate ligand H_8TDPEPE leads to a fluorescent material with a near-dark state. Immobilization of the ligand in the rigid structure also unexpectedly causes significant strain. We used DFT calculations to estimate the ligand strain energies in our and all other topologically related materials and correlated these with empirical structural descriptors to derive general rules for trapping molecules in high-energy conformations within MOFs. These studies portend possible applications of MOFs for studying fundamental concepts related to conformational locking and its effects on molecular reactivity and chromophore photophysics.

Metal–organic frameworks (MOFs) containing fluorescent building blocks have received considerable attention, primarily because of their potential utility in sensing applications.[1−3] The design of MOF-based sensors, especially for detecting gaseous analytes, presents two important advantages. First, MOFs have high internal surface areas and can therefore concentrate analytes to levels high above those in the surrounding atmosphere. This eliminates the need for sample pretreatment[4] and can lead to much smaller detection levels than otherwise available.[5] Second, the high degree of structural and chemical tunability in MOFs can in principle afford unprecedented selectivity either through size-exclusion or chemical interactions.[3] These features have led to the discovery of a range of new porous fluorescent and phosphorescent sensing materials,[6−10] but important challenges related mainly to signal transduction must be addressed to make MOF-based sensing devices competitive with state-of-the-art alternatives.

In luminescence-based sensors, signal transduction is achieved by detecting a change in the intensity or the wavelength of the luminescent signal. In MOFs, analyte molecules typically quench the excited states of lanthanide ions or fluorescent linkers, thereby turning off or reducing the luminescence intensity of the parent material. More desirable and easily detectable are *turn-on* mechanisms, where the presence of the analyte triggers either an increase in the luminescence intensity (preferably from a completely dark "off" state to a highly emissive one) or a shift in the emission wavelength.

To address the challenge of designing turn-on fluorescent MOF-based sensors, we turned to a class of fluorophores whose innate low-frequency vibrational modes, such as phenyl ring torsions and C=C twists, efficiently quench excited states internally, resulting in nonemissive default states.[11] Fluorescence in such molecules is turned on when the low-frequency vibrational quenching modes are eliminated. This is most frequently achieved through intermolecular steric interactions in the solid or colloidal state and is known as aggregation-induced emission (AIE).[12] We recently showed that AIE-type chromophores such as tetraphenylethylene (TPE) can also become fluorescent when the phenyl ring torsion is blocked by incorporation in a rigid MOF.[13] However, although the emission maxima *shifted* in the presence of analytes in the TPE-derived Zn_2(TCPE) [H_4TCPE = tetrakis(4-carboxyphenyl)ethylene], this material was fluorescent even in the absence of guest molecules and was therefore not a full turn-on sensor. We confirmed that phenyl ring torsion, which we hoped would quench the fluorescence in the guest-free material, had an intrinsic barrier that was already too high, rendering the material fluorescent even in the absence of analytes.[14] Clearly, a reduction in this internal torsional potential (ITP)[15] was necessary to obtain the darker off state characteristic of AIE-type sensors.

With an eye toward decreasing the barrier to phenyl ring torsion to provide a fluorescent MOF with a default dark off state, we have designed and synthesized an ethynyl-extended TPE-based ligand and incorporated it into a zinc-based MOF. Despite the rigidity of the MOF lattice, the new ligand shows a drastically reduced barrier to phenyl ring torsion and thereby a much lower fluorescence quantum yield compared with Zn_2(TCPE) and an almost perfect off ground state. Unexpectedly, the MOF lattice also locks the new ligand in a highly strained conformation with a strain energy (SE) rivaling those of fullerenes, highlighting a new potential avenue for fundamental studies in MOFs related to conformational locking.

The new ligand, tetrakis[4-(3,5-dicarboxyphenylethynyl)-phenyl]ethylene (H_8TDPEPE) (Figure 1), was conceived to minimize the torsional barrier for phenyl ring flipping in the central TPE core [Figure S1 in the Supporting Information (SI)] and is inspired from molecular rotors.[15] The most salient design features in H_8TDPEPE are the *p*-ethynyl groups extending from the phenyl rings in the TPE core; these exhibit cylindrical symmetry and are known to promote almost

Received: October 18, 2012
Published: November 19, 2012

dx.doi.org/10.1021/ja3103154 | J. Am. Chem. Soc. 2012, 134, 19596–19599

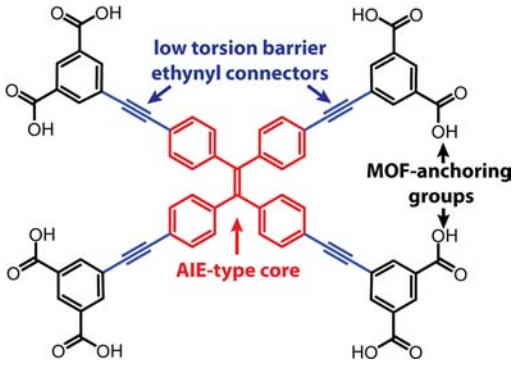

Figure 1. Molecular structure and design features of H_8TDPEPE.

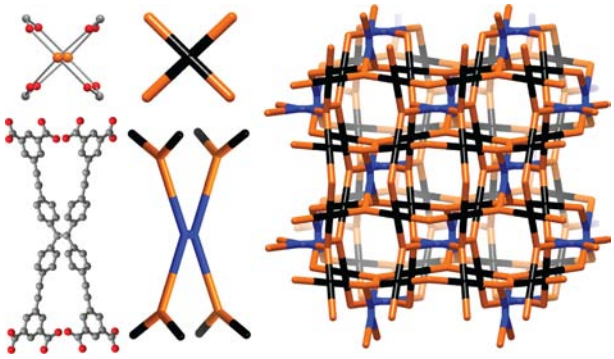

Figure 2. The 3,3,4-connected structure of **1**. Orange, red, and gray spheres represent Zn, O, and C atoms, respectively. H atoms and solvent molecules have been removed for clarity.

barrierless torsional motion for vicinal phenyl rings.[16] The ligand is terminated with isophthalate anchoring points, which were chosen because they have been the basis for some of the most porous MOFs reported to date.[17−19]

H_8TDPEPE was synthesized in six steps (Scheme S1 in the SI). The reaction of H_8TDPEPE with $Zn(NO_3)_2{\cdot}6H_2O$ at 75 °C for 1 day produced yellow crystals of $[Zn_4(TDPEPE)(H_2O)_4(DEF)_4]{\cdot}(H_2O)_3(DEF)_{9.5}$ (**1**) (DEF = *N*,*N*-diethylformamide).[20] X-ray diffraction (XRD) analysis of a crystal of **1** revealed a structure composed of paddlewheel $Zn_2(O_2C)_4$ secondary building units (SBUs) bridged by $TDPEPE^{8-}$ ligands into a three-dimensional 3,3,4-connected net with *tbo* topology[17,21,22] and Schläfli symbol $\{7^2.8^2.11^2\}\{7^2.8\}\{7^3\}_2$[23] (Figure 2).

Importantly, the centroid−centroid distance between phenyl rings on neighboring TPE cores in **1** is 10.24(1) Å (Figure S2). This value is sufficiently large to prevent intermolecular Ph···Ph (and Ph−H···Ph) interactions, which are responsible for fluorescence turn-on in *molecular* AIE aggregates.[24] Compound **1** is only weakly fluorescent and exhibits ligand-based emission with a maximum centered at 512 nm, which is blue-shifted by only 18 nm relative to that of the free ligand (Figure S3). Importantly, the fluorescence quantum yield (Φ_{fl}) of 9% observed for **1** is significantly lower than that observed for $[Zn_2(TCPE)(DEF)_2]{\cdot}DEF$[14] (35%),[25] wherein electronic factors contribute to a higher ITP (see above). Although the Φ_{fl} values of both MOFs are likely reduced by vibrational motions in the solvent molecules, the fluorescence lifetime of 3.87 ns observed in **1**[25] is comparable to that observed in the TCPE-based MOF, suggesting that dynamic quenching effects have similar contributions in the two materials. We thus

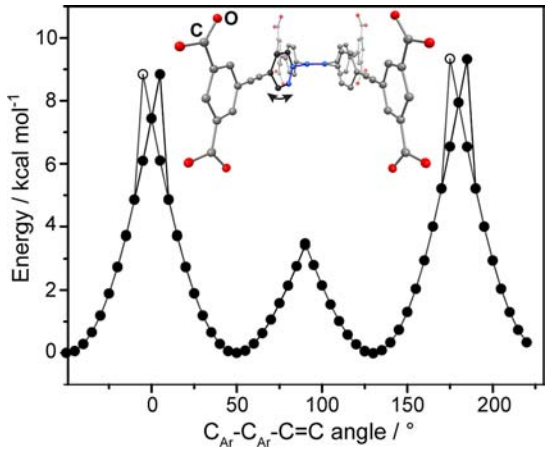

Figure 3. DFT-calculated ITP in H_8TDPEPE with the O atom coordinates fixed to those found in **1** in order to mimic the geometrical constraints imposed by the MOF lattice. The solid lines with black circles indicate the lowest-energy surfaces constructed from conrotatory (●) and disrotatory (○) ring-flip motions.

attribute the remarkable reduction of 26% in Φ_{fl} and the presence of the nearly dark off state in **1** to relaxed torsional motion of the phenyl rings in the TPE core, as originally designed.

To substantiate the hypothesis that the quenching of the fluorescence in **1** is due to a lower barrier for phenyl ring torsion in the TPE core, we used density functional theory (DFT) to calculate the ITP for the phenyl rings in $TDPEPE^{8-}$ constrained within **1** ($TDPEPE^{8-}\subset$**1**). The calculated activation barrier was found to be 9 kcal/mol (Figure 3), which is notably lower than that calculated for $[Zn_2(TCPE)(DEF)_2]{\cdot}2DEF$ (12 kcal/mol)[14] and only 3 kcal/mol larger than the barrier calculated for ring flipping in free TPE.[26] Because TPE itself is nonemissive, the very low activation barrier for phenyl ring flipping is consistent with the almost complete quenching of fluorescence in **1**.

To assess the viability of **1** as a porous turn-on sensing material, as-synthesized crystals were subjected to both supercritical CO_2 drying and typical vacuum-heating desolvation techniques. However, both approaches caused the irreversible formation of a crystalline yet nonporous phase (Figure S4). Because MOFs with Cu-based paddlewheels are more stable than their Zn analogues,[27,28] we also attempted but failed to access a Cu analogue of **1** both solvothermally and by postsynthetic ion metathesis.[29]

In searching for clues for the surprising instability of **1** relative to other MOFs with paddlewheel SBUs, we found a striking conformational difference between $TDPEPE^{8-}\subset$**1** and DFT-optimized H_8TDPEPE. The centroid−centroid distances between isophtalate units are 12.44 and 8.24 Å in free H_8TDPEPE and $TDPEPE^{8-}\subset$**1**, respectively (Figure S5). The SE associated with the latter is 383.7 kcal/mol, which corresponds to an average per-bond SE of 4.31 kcal/mol. For comparison, the estimated SE for the less bulky $TCPE^{4-}\subset Zn_2(TCPE)$[14] is only 51.6 kcal/mol (1.26 kcal/mol per bond), 7 times lower than that in **1**.

It seemed plausible that the mechanical instability of **1** was the direct result of the enormous strain on its constituent ligand; more broadly, this suggested that *the influence of strain on MOF stability is part of a general phenomenon that has hitherto gone unnoticed in MOFs*, especially in those with large ligands.

dx.doi.org/10.1021/ja3103154 | J. Am. Chem. Soc. 2012, 134, 19596−19599

Table 1. DFT-Calculated SEs for Selected Ligands⊂MOFs

MOF[a]	SE/SE per bond (kcal/mol)	$\kappa_{ligand}/\kappa_{MOF}$[c]
$Mn_3[(Mn_4Cl)_3(TPT\text{-}3tz)_8]_2$[32]	21.5/0.48	–
$(Zn_4O)_4(BTE)_4(BPDC)_3$[b] (MOF-210)[30]	34.0/0.81	–
	35.0/0.83	–
	41.7/0.99	–
$Zn_4O(BTE)_2$ (MOF-180)[30]	51.8/1.23	–
$Cu_4(TDM)(H_2O)_4$ (PCN-26)[22]	74.8/1.25	1.5/1.7
$Cu_4(MTBD)(H_2O)_4$ (NOTT-140)[21]	75.5/0.94	2.2[33]/1.5
$Zn_4O(BBC)_2$ (MOF-200)[30]	111.9/1.96	–
$Cu_4(PTMT)(H_2O)_4$[38]	113.9/1.73	1.2/1.4
$Cu_4(BTTCD)(H_2O)_4$ (PCN-80)[17]	201.0/1.99	1.3/1.1
$Cu_4(BTMPT)(H_2O)_4$[38]	211.8/2.08	1.0/1.4
$Cu_3(TCAEPEB)(H_2O)_3$ (NU-100)[19]	215.4/2.76	–
1	**383.7/4.31**	2.3/1.5

[a]BTE = 4,4′,4″-[benzene-1,3,5-triyl-tris(ethyne-2,1-diyl)]tribenzoate; BPDC = biphenyl-4,4′-dicarboxylate; TDM = tetrakis[(3,5-dicarboxyphenyl)oxamethyl]methane; MTBD = 4′,4‴,4⁗,4⁗′-methanetetrayl-tetrakis(biphenyl-3,5-dicarboxylate); BBC = 4,4′,4″-[benzene-1,3,5-triyl-tris(benzene-4,1-diyl)]tribenzoate; PTMT = 5,5′,5″,5‴-[1,2,4,5-phenyltetramethoxy]tetraisophthalate; BTMPT = 5,5′,5″,5‴-[1,2,4,5-benzenetetrakis(4-methyleneoxyphenylazo)]tetraisophthalate; TPT-3tz =2,4,6-tri-*p*-(tetrazol-5-yl)phenyl-*s*-triazine; BTTCD = 9,9′,9″,9‴-[(1,1′-biphenyl)-3,3′,5,5′-tetrayl]tetrakis(9*H*-carbazole-3,6-dicarboxylate); TCAEPEB = 1,3,5-tris{[4-(3,5-dicarboxyphenylethynyl)phenyl]ethynyl}benzene. [b]Values are given for three independent conformations of the ligand in MOF-210. [c]κ_{ligand} and κ_{MOF} are equal to d_1/d_2 for the DFT-optimized ligand and the ligand in Ligand⊂MOF, respectively. See Figure S18 for details on deriving this ratio.

To test this hypothesis, we calculated the SEs of constituent ligands in the respective conformations imposed by different MOFs with large surface areas and high-quality crystal structures.[19,30−32] The results of these calculations are listed in Table 1 (also see Figures S9−S17). NU-100, MOF-180, and MOF-210 contain hexatopic or tritopic ligands with ethynyl spacers that, like H_8TDPEPE, can provide additional flexibility and facilitate ligand bending and distortion. According to our calculations, the most strained of these ligands is H_6TCAEPEB in NU-100; its SE of 215.4 kcal/mol amounts to 2.76 kcal/mol per bond, which is still ∼1.8 times lower than that in TDPEPE^{8-}⊂**1**. We also found that tritopic ligands had lower per-bond SEs than either TDPEPE^{8-}⊂**1** or the ligand in NU-100 because their idealized geometries map directly onto the faces of the polyhedra in their respective networks. Notably, these calculations suggested that the strain in TDPEPE^{8-}⊂**1** is not strictly related to ligand size or functional groups but could instead be the result of the specific geometric requirements of nets with the *tbo* topology.

Indeed, structural analysis of known MOFs with the *tbo* topology revealed that the intra- and interarm inter-SBU distances (red and blue lines, respectively, in Figure 4a,b) define a rhombus and therefore *must be equal* regardless of the ligand. The octacarboxylate ligands forming these MOFs can be described in a general way by two distances d_1 and d_2 (Figures 4c and S18.) Because the dimension of the rhombus is proportional to d_2, one can predict empirically that significant strain should be imposed on ligands within *tbo* nets when the ratio $\kappa = d_1/d_2$ in the free ligand is much larger than ∼1.5. Higher κ values should increase the SE and consequently decrease the MOF stability. This suggests that there is a threshold value of κ above which tbo MOFs cannot be permanently porous. This threshold value will likely correlate with the strength of the coordination bond involved in the formation of the MOF, with Zn−O bonds allowing lower κ threshold values than Zr−O and Al−O bonds, for instance.

This empirical rule was indeed verified by calculations of SEs in known MOFs with the *tbo* topology. Not surprisingly, with κ = 2.3, TDPEPE^{8-}⊂**1** has the highest SE. The other κ values ranged from 1.0 to 1.5.[33] Clearly, high κ values are detrimental to permanent porosity. However, there are situations where the deliberate isolation of molecules in highly strained conformations can impart new reactivity[34] or shed light on photophysical properties[35] relevant to organic photovoltaics, for instance. Our empirical rule states that one can predict high SEs in ligands where κ is maximized. Strategies for maximizing κ could include (1) the use of high-connectivity ligands that are likely to yield three-dimensional nets; (2) the use of only sp and sp^2 hybridization to construct rigid ligands with high potential for strain; and (3) the use of rectangularly extended ligands that maximize d_1, which can be checked by molecular mechanics. Although small molecules can show higher SEs than TDPEPE^{8-}⊂**1** [e.g., C_{60} (SE = 484 kcal/mol, 5.38 kcal/mol

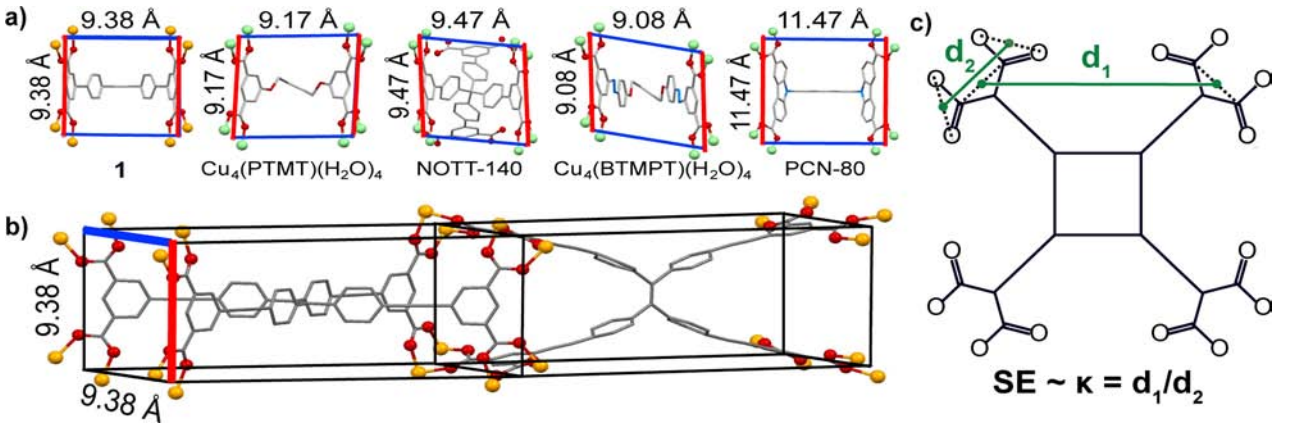

Figure 4. (a) Portions of the X-ray crystal structures of known MOFs with the *tbo* topology. Red and blue lines represent the intra- and interarm inter-SBU distances, respectively. Orange, green, red, gray, and blue nodes represent Zn, Cu, O, C, and N atoms, respectively. Ligand names and MOF formulas are given in Table 1. (b) Portion of the X-ray crystal structure of **1** evidencing the strain in TDPEPE^{8-}⊂1; solid black lines are given as visual guides. (c) Generalized scheme of an octacarboxylate ligand described by the intra- and interarm intercarboxylate distances d_1 and d_2.

dx.doi.org/10.1021/ja3103154 | J. Am. Chem. Soc. 2012, 134, 19596−19599

per bond)[36] and [8]cycloparaphenylenes (SE = 74 kcal/mol, 1.32 kcal/mol per bond)[37]], we emphasize that the SEs observed in Ligands⊂MOFs are enforced by conformational locking via coordination bonds and are not native to the ligands themselves. In other words, the high-energy locked conformation contains "extractable" or "accessible" potential energy.

The foregoing results show that design principles adapted from molecular rotors can be used for the rational construction of a luminescent MOF with a near-dark off state, a first step toward high-surface-area turn-on fluorescent sensors. They also unexpectedly reveal that ligands can be locked in high-energy conformations within MOFs through topological design. These findings may be used to make empirical predictions of the stabilities of certain MOFs toward evacuation, a hitherto purely experimental endeavor, and to interrogate the fundamental properties of molecules under mechanical stress.

■ ASSOCIATED CONTENT

Ⓢ Supporting Information

Experimental details, X-ray structure refinement table, NMR spectra, DFT-calculated potential energy surfaces, and optimized ligand geometries. This material is available free of charge via the Internet at http://pubs.acs.org.

■ AUTHOR INFORMATION

Corresponding Author

mdinca@mit.edu

Author Contributions

[†]N.B.S. and A.F.C. contributed equally.

Notes

The authors declare no competing financial interest.

■ ACKNOWLEDGMENTS

This work was supported as part of the Center for Excitonics, an Energy Frontier Research Center funded by the U.S. Department of Energy, Office of Science, Office of Basic Energy Sciences under Award DE-SC0001088 (MIT). The authors thank Nicholas Thompson, Phil Reusswig, and Prof. Mark Baldo for help with the Φ_{fl} measurements and use of the integrating sphere. NSF provided instrument support to the DCIF and the single-crystal XRD facility at MIT (Grants CHE-9808061, DBI-9729592, CHE-0946721).

■ REFERENCES

(1) Allendorf, M. D.; Bauer, C. A.; Bhakta, R. K.; Houk, R. J. T. *Chem. Soc. Rev.* **2009**, *38*, 1330.

(2) Cui, Y.; Yue, Y.; Qian, G.; Chen, B. *Chem. Rev.* **2012**, *112*, 1126.

(3) Kreno, L. E.; Leong, K.; Farha, O. K.; Allendorf, M.; Van Duyne, R. P.; Hupp, J. T. *Chem. Rev.* **2012**, *112*, 1105.

(4) Gu, Z.; Wang, G.; Yan, X. *Anal. Chem.* **2010**, *82*, 1365.

(5) Robinson, A. L.; Stavila, V.; Zeitler, T. R.; White, M. I.; Thornberg, S. M.; Greathouse, J. A.; Allendorf, M. D. *Anal. Chem.* **2012**, *84*, 7043.

(6) An, J.; Shade, C. M.; Chengelis-Czegan, D. A.; Petoud, S.; Rosi, N. L. *J. Am. Chem. Soc.* **2011**, *133*, 1220.

(7) Lan, A.; Li, K.; Wu, H.; Olson, D. H.; Emge, T. J.; Ki, W.; Hong, M.; Li, J. *Angew. Chem., Int. Ed.* **2009**, *48*, 2334.

(8) Xie, Z.; Ma, L.; deKrafft, K. E.; Jin, A.; Lin, W. *J. Am. Chem. Soc.* **2010**, *132*, 922.

(9) Takashima, Y.; Martínez, V. M.; Furukawa, S.; Kondo, M.; Shimomura, S.; Uehara, H.; Nakahama, M.; Sugimoto, K.; Kitagawa, S. *Nat. Commun.* **2011**, *2*, 168.

(10) Stylianou, K. C.; Heck, R.; Chong, S. Y.; Bacsa, J.; Jones, J. T. A.; Khimyak, Y. Z.; Bradshaw, D.; Rosseinsky, M. J. *J. Am. Chem. Soc.* **2010**, *132*, 4119.

(11) Tong, H.; Hong, Y.; Dong, Y. Y.; Häussler, M.; Li, Z.; Lam, J. W. Y.; Sung, H. H.-Y.; Williams, I. D.; Tang, B. Z. *J. Phys. Chem. B* **2007**, *111*, 11817.

(12) Hong, Y.; Lam, J. W. Y.; Tang, B. Z. *Chem. Soc. Rev.* **2011**, *40*, 5361.

(13) Shustova, N. B.; McCarthy, B. D.; Dincă, M. *J. Am. Chem. Soc.* **2011**, *133*, 20126.

(14) Shustova, N. B.; Ong, T.-C.; Cozzolino, A. F.; Michaelis, V. K.; Griffin, R. G.; Dincă, M. *J. Am. Chem. Soc.* **2012**, *134*, 15061.

(15) Kottas, G. S.; Clarke, L. I.; Horinek, D.; Michl, J. *Chem. Rev.* **2005**, *105*, 1281.

(16) Okuyama, K.; Hasegawa, T.; Ito, M.; Mikami, N. *J. Phys. Chem.* **1984**, *88*, 1711.

(17) Lu, W.; Yuan, D.; Makal, T.; Li, J.-R.; Zhou, H.-C. *Angew. Chem., Int. Ed.* **2012**, *51*, 1580.

(18) Farha, O. K.; Wilmer, C. E.; Eryazici, I.; Hauser, B. G.; Parilla, P. A.; O'Neill, K.; Sarjeant, A. A.; Nguyen, S. T.; Snurr, R. Q.; Hupp, J. T. *J. Am. Chem. Soc.* **2012**, *134*, 9860.

(19) Farha, O. K.; Yazaydın, A. Ö.; Eryazici, I.; Malliakas, C. D.; Hauser, B. G.; Kanatzidis, M. G.; Nguyen, S. T.; Snurr, R. Q.; Hupp, J. T. *Nat. Chem.* **2010**, *2*, 944.

(20) Crystallographic data for **1** are shown in Table S1 in the SI.

(21) Tan, C.; Yang, S.; Champness, N. R.; Lin, X.; Blake, A. J.; Lewis, W.; Schröder, M. *Chem. Commun.* **2011**, *47*, 4487.

(22) Zhuang, W.; Yuan, D.; Liu, D.; Zhong, C.; Li, J.-R.; Zhou, H.-C. *Chem. Mater.* **2012**, *24*, 18.

(23) The topological assignment for the network of **1** was performed with TOPOS. See: Blatov, V. A. *IUCr CompComm Newsl.* **2006**, *7*, 4. Also see: http://www.topos.ssu.samara.ru.

(24) As verified by a Cambridge Crystallographic Database search in October 2012.

(25) Φ_{fl} values for H_4TCPE, Zn_2(TCPE)$(DEF)_2$, and Zn_2(TCPE) were remeasured using an integrating sphere and adjusted from the previously reported values.[13] The updated values are 47, 35, and 39%, respectively.

(26) Block, J.; Ertl, G.; Haul, R.; Wedler, G. *Ber. Bunsen-Ges. Phys. Chem.* **1971**, *75*, 1665.

(27) Feldblyum, J. I.; Liu, M.; Gidley, D. W.; Matzger, A. J. *J. Am. Chem. Soc.* **2011**, *133*, 18257.

(28) Tan, K.; Nijem, N.; Canepa, P.; Gong, Q.; Li, J.; Thonhauser, T.; Chabal, Y. J. *Chem. Mater.* **2012**, *24*, 3153.

(29) Brozek, C. K.; Dincă, M. *Chem. Sci.* **2012**, *3*, 2110.

(30) Furukawa, H.; Ko, N.; Go, Y. B.; Aratani, N.; Choi, S. B.; Choi, E.; Yazaydin, A. O.; Snurr, R. Q.; O'Keeffe, M.; Kim, J.; Yaghi, O. M. *Science* **2010**, *329*, 424.

(31) Farha, O. K.; Eryazici, I.; Jeong, N. C.; Hauser, B. G.; Wilmer, C. E.; Sarjeant, A. A.; Snurr, R. Q.; Nguyen, S. T.; Yazaydin, A. Ö.; Hupp, J. T. *J. Am. Chem. Soc.* **2012**, *134*, 15016.

(32) Dincă, M.; Dailly, A.; Tsay, C.; Long, J. R. *Inorg. Chem.* **2008**, *47*, 11.

(33) Although the ligand in NOTT-140 (Figure S11) has $\kappa_{ligand} = 2.2$, it has a low SE (75.45 kcal/mol) because its arms can adopt low-energy conformations by twisting around a single bond, a conformational change with a relatively flat potential energy surface.

(34) Takezawa, H.; Murase, T.; Fujita, M. *J. Am. Chem. Soc.* **2012**, *134*, 17420.

(35) Huang, H.; Chen, Z.; Ortiz, R. P.; Newman, C.; Usta, H.; Lou, S.; Youn, J.; Noh, Y.-Y.; Baeg, K.-J.; Chen, L. X.; Facchetti, A.; Marks, T. *J. Am. Chem. Soc.* **2012**, *134*, 10966.

(36) Haddon, R. C. *Science* **1993**, *261*, 1545.

(37) Xia, J.; Bacon, J. W.; Jasti, R. *Chem. Sci.* **2012**, *3*, 3018.

(38) Eubank, J. F.; Mouttaki, H.; Cairns, A. J.; Belmabkhout, Y.; Wojtas, L.; Luebke, R.; Alkordi, M.; Eddaoudi, M. *J. Am. Chem. Soc.* **2011**, *133*, 14204.